

Application of Single Molecule Förster Resonance Energy Transfer to Protein Folding

Benjamin Schuler

Summary

Protein folding is a process characterized by a large degree of conformational heterogeneity. In such cases, classical experimental methods yield only mean values, averaged over large ensembles of molecules. The microscopic distributions of conformations, trajectories, or sequences of events often remain unknown, and with them the underlying molecular mechanisms. Signal averaging can be avoided by observing individual molecules. A particularly versatile method is highly sensitive fluorescence detection. In combination with Förster resonance energy transfer, distances and conformational dynamics can be investigated in single molecules. This chapter introduces the practical aspects of applying this method to protein folding.

Key Words: Protein folding; fluorescence spectroscopy; single molecule detection; Förster resonance energy transfer; FRET; diffusion; folding trajectories.

1. Introduction

The direct investigation of the folding of single protein molecules has only become feasible by means of new methods such as atomic force microscopy (AFM) (1,2) and optical single molecule spectroscopy (3–9). These techniques offer a fundamental advantage beyond mere fascination for the direct depiction of molecular processes: they can resolve and quantify the properties of individual molecules or subpopulations inaccessible in classical ensemble experiments, where the signal is an average over many particles. Fluorescence spectroscopy is a particularly appealing technique, owing to its extreme sensitivity and versatility (5,10,11). In combination with Förster resonance energy transfer (FRET) (12–14), it enables us to investigate intramolecular distance distributions and conformational dynamics of single proteins. Time-resolved ensemble FRET can also be used to separate subpopulations and to obtain information on distance

distributions (15), but data interpretation is typically less model independent (16). For kinetic ensemble studies, the reactions need to be synchronized, which is often difficult. An impressive example for the power of single molecule studies is single channel recording, which now dominates the study of ion channels and has revealed countless mechanisms that could not be obtained from ensemble experiments (17).

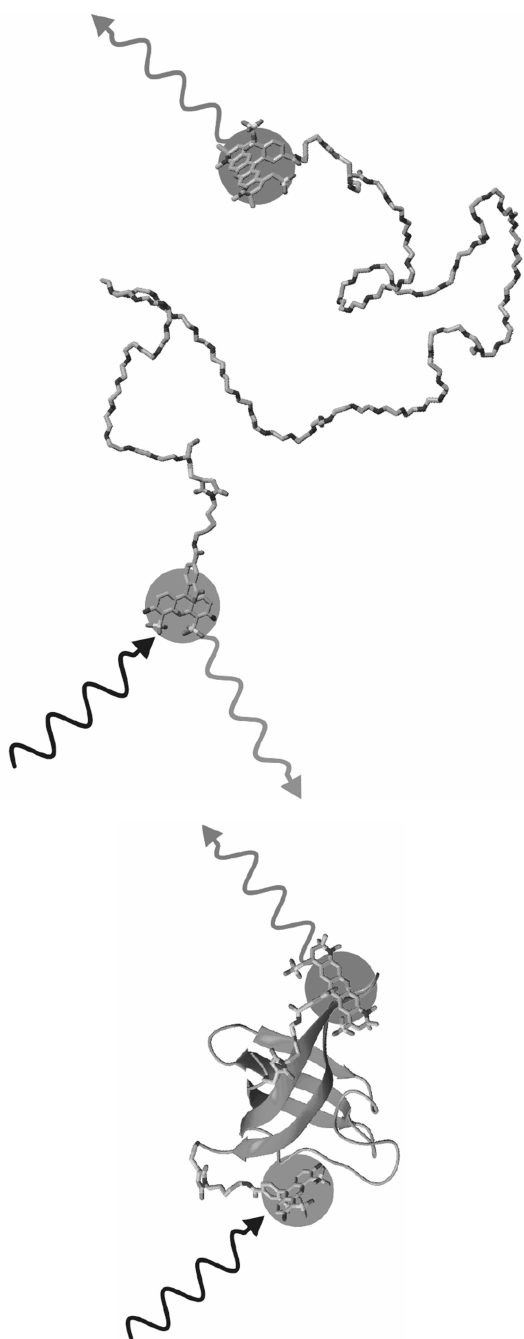
Currently, the two most common single molecule methods to study protein folding are AFM and single pair FRET (18). The first observations of the unfolding of single protein molecules were made using AFM (1) and laser tweezers (19). Soon the first experiments using fluorescence followed (20–22), which demonstrated the potential of single molecule spectroscopy for separating subpopulations and for obtaining dynamic information. Since then, single molecule spectroscopy has been used to identify the equilibrium collapse of unfolded protein under near-native conditions (23), to study folding kinetics (24), the dimensions of denatured proteins (25), and to investigate previously inaccessible parameters of the free energy surface of protein folding (23). Work on immobilized protein molecules has also allowed the study of reversible folding (26), and has even enabled the direct observation of folding and unfolding trajectories (27,28). For a recent review of the progress, concepts and theory of single molecule spectroscopy of protein folding, see ref. 29.

The basic idea of a protein folding experiment using FRET is very simple (**Fig. 1**): a donor dye and an acceptor dye are attached to specific residues of a protein. If a folded protein molecule resides in the volume illuminated by the focused laser beam, excitation of the donor dye results in rapid energy transfer to the acceptor dye because the dyes are in close proximity. Consequently, the majority of the fluorescence photons are emitted by the acceptor. Upon unfolding of the protein, the average distance between the donor and acceptor dyes will typically increase. As a result, the energy transfer rate is decreased, and the fraction of photons emitted by the acceptor is lower. The changes in fluorescence intensity from donor and acceptor can thus be used to distinguish between different conformational states of a protein.

1.1. Förster Resonance Energy Transfer

The quantitative relationship between the probability of transfer—the transfer efficiency—and the inter-dye distance is given by a theory developed by

Fig. 1. (*Opposite page*) Schematic structures of folded and unfolded protein labeled with donor (Alexa 488) and acceptor (Alexa 594) dyes. (A) Folded CspTm, a five-stranded, 66-residue β -barrel protein (PDB-code 1G6P) (75), (B) unfolded CspTm. A blue laser excites the green-emitting donor dye, which can transfer excitation energy to the red-emitting acceptor dye.



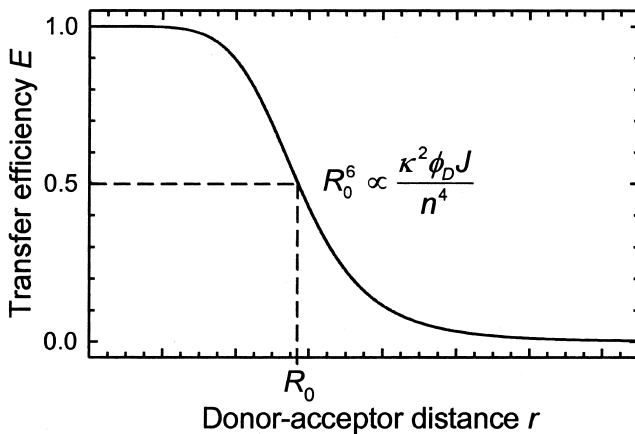


Fig. 2. Distance dependence of the transfer efficiency according to Förster theory (**Eq. 1**). The Förster radius R_0 is calculated according to **Eq. 2**. Owing to the characteristic $1/r^6$ dependence, the transfer efficiency is most sensitive for distance changes in the vicinity of R_0 .

Theodor Förster in the 1940s (**12**). According to Förster's theory, the transfer efficiency, E , for the dipole–dipole coupling between a donor and an acceptor chromophore depends on the inverse sixth power of the inter-dye distance, r :

$$E = \frac{R_0^6}{R_0^6 + r^6} \quad (1)$$

where R_0 is the Förster radius, the characteristic distance that results in a transfer efficiency of 50% (**Fig. 2**). Because of the strong distance dependence of the efficiency, FRET can be used as a “spectroscopic ruler” on molecular length scales, typically between 2 and 10 nm. R_0 is calculated as (*see Note 1*)

$$R_0^6 = \frac{9000 \ln 10 \kappa^2 Q_D J}{128\pi^5 n^4 N_A} \quad (2A)$$

where J is the overlap integral, Q_D is the donor's fluorescence quantum yield, n the refractive index of the medium between the dyes, and N_A is Avogadro's number (**12,30**). The orientational factor is defined as $\kappa^2 = (\cos \Theta_T - 3 \cos \Theta_D \cos \Theta_A)^2$, where Θ_T is the angle between the donor emission transition dipole moment and the acceptor absorption transition dipole moment, Θ_D and Θ_A are the angles between the donor–acceptor connection line and the donor emission and the acceptor absorption transition moments, respectively. κ^2 varies between 0 and 4, but complete averaging of the relative orientation of the chromophores during the excited state lifetime of the donor results in a value of two-thirds the

value most frequently used in practice (however, *see Subheading 3.3.*). Q_D and n need to be measured (*see Note 2*), and J is calculated from the normalized donor emission spectrum $f_D(\lambda)$ and the molar extinction coefficient of the acceptor $\epsilon_A(\lambda)$ according to:

$$J = \int_0^{\infty} f_D(\lambda) \epsilon_A(\lambda) \lambda^4 d\lambda \quad (2B)$$

The accuracy of the calculation is ultimately limited by n , which is often nonuniform and difficult to estimate for a protein (but probably very close to n of the solvent for an unfolded protein), and ϵ_A , which cannot easily be determined independently and is provided by the manufacturer with an uncertainty of at least a few percent. Fortunately, the influence of such uncertainties is moderated by the fact that R_0 depends only on the sixth root of n^{-4} and J respectively, of these quantities (**Eq. 2A**).

Experimentally, transfer efficiencies can be determined in a variety of ways (**30**), but for single molecule FRET, two approaches have proven particularly useful. One is the measurement of the number of photons (**31**) emitted from the donor and the acceptor chromophores, n_D and n_A , respectively, and the calculation of the transfer efficiency according to:

$$E = \frac{n_A}{n_A + n_D} \quad (3)$$

where the numbers of photons are corrected for the quantum yields of the dyes, direct excitation of the acceptor, the detection efficiencies of the optical system in the corresponding wavelength ranges, and the crosstalk between the detection channels (*see Note 3*). A second approach to measure E , which can be combined with the first (**32**), is the determination of the fluorescence lifetime of the donor in the presence (τ_{DA}) and absence (τ_D) of the acceptor, yielding the transfer efficiency as:

$$E = 1 - \frac{\tau_{DA}}{\tau_D} \quad (4)$$

Frequently, we have to consider a distance distribution instead of a single distance, especially in unfolded proteins. If information about the distance distribution is available from simulations or independent experiments, it can be included in the analysis (**33**). In general, it is important to be aware of the different averaging regimes, because the time-scales of both conformational dynamics of the protein and re-orientational dynamics of the dyes influence the way the resulting transfer efficiency has to be calculated (**30,33**).

1.2. Outline of the Procedures

Performing a single molecule FRET experiment on protein folding requires several steps. First, protein samples have to be prepared for labeling, either by chemical synthesis or by recombinant expression in combination with site-directed mutagenesis. After identifying a suitable dye pair with the Förster radius in the desired range, the fluorophores need to be attached to the protein as specifically as possible to avoid chemical heterogeneity. The equilibrium and kinetic properties of the labeled protein should then be measured in ensemble FRET experiments and compared directly to unlabeled protein to ensure that the folding mechanism is not altered. For control experiments, it is helpful to prepare reference molecules, such as polyproline peptides or double-stranded DNA, with the same chromophores as the protein. After customizing the instrument for the sample, data can either be taken on freely diffusing molecules, or on immobilized molecules if observation times greater than a few milliseconds are desired. Finally, the data need to be processed to distinguish signal from background, to identify fluorescence bursts in diffusion experiments, and to calculate transfer efficiencies and the resulting distance changes.

2. Materials

2.1. Instrumentation

Considering that most molecular biologists or biochemists will not attempt to build their own single molecule instrument, it will be assumed in the following that a suitable system is already accessible, and instrument design will not be described. The details of single molecule instrumentation can be found in several recent reviews (5,10,34,35). An important development for the wide application of single molecule methods to the study of biomolecules is the recent availability of comprehensive commercial instrumentation (36).

Experimental setups for single molecule FRET typically involve either confocal excitation and detection using a pulsed or continuous wave (cw) laser and avalanche photodiodes (APDs), or wide-field microscopy with two-dimensional (2D) detectors, such as intensified or electron-multiplying CCD cameras. Wide-field imaging allows the collection of data from many single molecules in parallel, albeit at lower time resolution and signal-to-noise ratio than in a confocal experiment using APDs. Imaging can be performed either via epi-illumination, where the exciting laser light is directed to the sample through the epi-illumination port of a conventional fluorescence microscope, or via evanescent field excitation, typically by total internal reflection of the excitation light at the water/glass interface, where the sample molecules are located.

Figure 3 shows a schematic with the main optical elements for confocal epifluorescence detection. A laser beam is focused with a high numerical aperture objective to a diffraction-limited focal spot that serves to excite the labeled

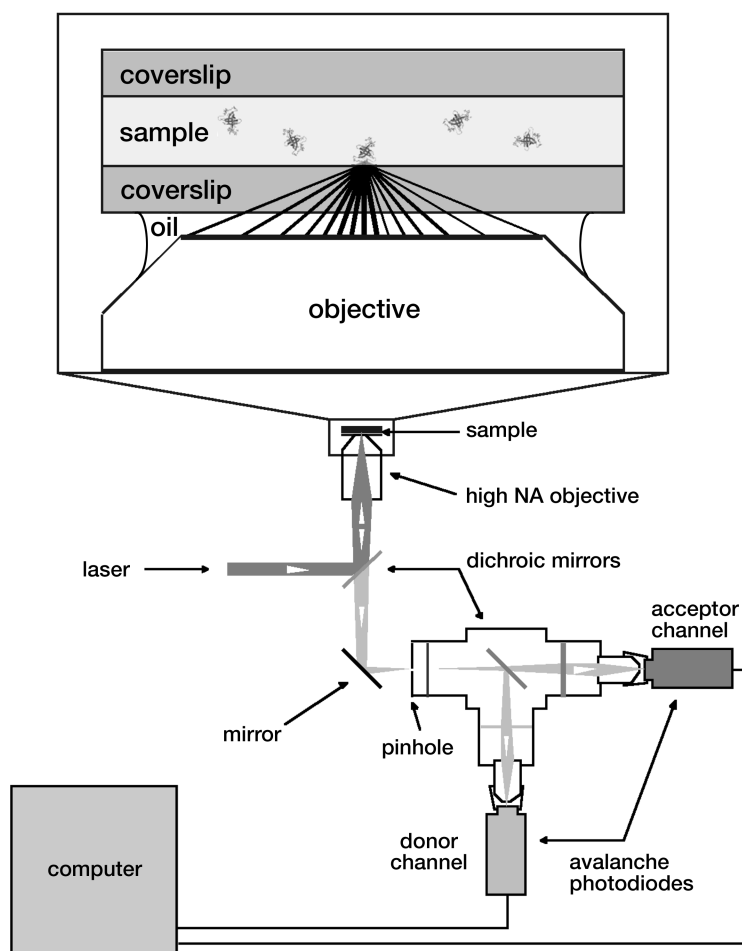


Fig. 3. Schematic of a confocal single molecule experiment on freely diffusing molecules (molecules not to scale). In this example, the signal is separated by wavelength into two detection channels corresponding to emission from donor and acceptor chromophores. With additional dichroic mirrors or polarizing beam splitters, the system can be extended to monitor polarization and/or emission from more dyes in parallel. In combination with a *xy*-stage, the system can be used for confocal imaging by sample scanning.

molecules. In the simplest experiment, the sample molecules are freely diffusing in solution at very low concentration, ensuring that the probability of two molecules residing in the confocal volume at the same time is negligible. When a molecule diffuses through the laser beam, the donor dye is excited and fluorescence from donor and acceptor is collected through the objective and gets focused onto the pinhole, a small aperture serving as a spatial filter. A dichroic

mirror finally separates donor and acceptor emission into the corresponding detectors, from where the data are collected with multichannel scalers or suitable counting cards. The setup can be extended to sorting photons by additional colors, e.g., if more than two chromophores are used (37,38), or by both wavelength and polarization (32,39). The system can be coupled to a piezo xy flexure stage for sample scanning, which allows the acquisition of fluorescence images and the reproducible positioning of the laser beam on individual molecules immobilized on the surface. Even better spatial separation than with confocal one-photon excitation can be achieved by two-photon excitation (40).

The advantage of observing freely diffusing molecules is that perturbations from surface interactions can largely be excluded, but the observation time is limited by the diffusion times of the molecules through the confocal volume. Typically, every molecule is observed for no more than a few milliseconds in the case of proteins. Alternatively, molecules can be immobilized on the surface and then observed for a more extended period of time, typically a few seconds, until one of the chromophores undergoes photodestruction. The complications in this case are interactions with the surface that can easily perturb the sensitive equilibrium of protein folding.

For sample design, especially for choosing the chromophores, it is important to be aware of the characteristics and limitations of the instrument, such as the laser lines available for excitation or the time resolution and signal-to-noise ratio achievable with the detectors. The lasers typically used range from simple cw systems with a single fixed wavelength to large, tunable, pulsed lasers that make a broad range of wavelengths accessible. With a pulsed source, fluorescence lifetimes become available in addition to intensities, which can provide additional information (39,41).

2.2. *Chemicals*

Obviously, single molecule fluorescence experiments make great demands on buffer preparation and sample purity. Even though a single molecule is always pure, researchers rarely have the means to distinguish sample molecules unequivocally from contaminants. Some solutes, e.g., denaturants or osmolytes, may be present at concentrations of several molar. Highest purity buffer substances are therefore strictly required. Common buffers, such as phosphate salts and Tris, can be obtained in excellent purity from most major suppliers as spectrophotometric grade chemicals, other substances only from more specialized sources (e.g., GdmCl and Tween-20 [Pierce Biotechnology, Rockford, IL]). As a general rule, all solutions have to be tested in the single molecule instrument for fluorescent impurities prior to use. Quartz-bidistilled water is recommended; water from ion exchanger water purification systems (“MilliQ”) is usually suitable, but needs to be monitored more regularly for contaminations.

Fluorophores for protein labeling can be obtained with a variety of reactive groups from several manufacturers, such as Molecular Probes/Invitrogen (Alexa Fluors), Amersham Biosciences (cyanine dyes), and others.

2.3. Chromatography

Purification of labeled proteins proceeds very much the same way as any other protein purification, but again, buffers should have very low fluorescence background. High-performance liquid chromatography (HPLC) or fast protein liquid chromatography (FPLC) systems with fluorescence and diode array absorption detectors can greatly simplify the identification of correctly labeled species.

3. Methods

3.1. Choosing the Fluorophores

Several criteria must be met by chromophores for single molecule FRET:

1. They must have suitable photophysical and photochemical properties, especially a large extinction coefficient ($\sim 10^5 \text{ M}^{-1}\text{cm}^{-1}$ or greater), a quantum yield close to 1, high photostability, a low triplet state yield, and small intensity fluctuations (which can result from intermittence, i.e., transitions between bright and dark states).
2. The absorption maximum of the donor chromophore must be close to a laser line available for excitation.
3. Good spectral separation of donor and acceptor emission is necessary to minimize direct excitation of the acceptor and to reduce crosstalk between the detection channels.
4. Acceptor absorption and donor emission spectra must give an overlap integral that results in a suitable Förster radius (calculated from Eq. 2). Keep in mind that the best sensitivity for distance changes can be obtained for distances close to R_0 .
5. The dyes must be available with suitable functional groups for specific protein labeling (typically succinimidyl esters for amino groups or maleimides for sulfhydryl groups).
6. The dyes must be sufficiently soluble in aqueous buffers, otherwise they may induce protein aggregation, a problem that has been minimized by the introduction of charged groups in many of the popular dyes (42,43).

Note that some of the fluorophores' properties may change on attachment to the protein. In many cases, it is thus advisable to screen a series of dye pairs. The most commonly used dyes are organic fluorophores developed specifically for sensitive fluorescence detection. Examples of common dye pairs are Cy3/Cy5 and Alexa 488/Alexa 594. Semiconductor quantum dots (44,45) are promising candidates because of their extreme photostability, but they are not yet available with single functional groups, so far they can only be used as donors because of their broad absorption spectra, and they are themselves of the size of a small protein, which increases the risk of interference with the folding process. As of today,

tryptophan, the amino acid most commonly used for fluorescence detection in proteins, is not suitable for single molecule detection (unless the molecule contains a very large number of tryptophan residues [46]) owing to the low photostability of the indole ring.

3.2. Protein Labeling

To our misfortune, protein chemistry has not made it easy for us to investigate polypeptides in single molecule experiments (with the exception of the family of fluorescent proteins [47,48]). Specific placement of fluorophores on the protein ideally requires groups with orthogonal chemistry. For simple systems, such as short peptides, sequences can be designed to introduce only single copies of residues with suitable reactive side chains (23,33). In chemical solid-phase peptide synthesis, protection groups and the incorporation of non-natural amino acids can be used to increase specificity, but for longer chains, chemical synthesis becomes inefficient and shorter chains have to be ligated (49) to obtain the desired product (22).

The production of proteins of virtually any size and sequence by heterologous recombinant protein expression is the method of choice to obtain very pure material in sufficiently large amounts for preparative purposes. But the number of functional groups that can be used for specific labeling is then very limited. Sufficiently specific reactivity in natural amino acids is only provided by the sulphydryl groups of cysteine residues, the ϵ -amino groups of lysine side chains, and the free α -amino group of the N-terminal amino acid. However, except for small peptides, the statistical and, therefore, often multiple occurrence of cysteine and especially lysine residues in one polypeptide prevents the specific attachment of labels. Increased specificity can be achieved by removing unwanted natural cysteines by site-directed mutagenesis or introducing cysteines with different reactivity owing to different molecular environments within the protein (50). Labeling is usually combined with multiple chromatography steps to purify the desired adducts. Alternative methods (51) are native chemical ligation of recombinantly expressed and individually labeled protein fragments or intein-mediated protein splicing (52), the specific reaction with thioester derivatives of dyes (53), puromycin-based labeling using in vitro translation (54), or introduction of non-natural amino acids (55). Most of the latter methods are not yet used routinely, are not openly available, or must be considered under development.

Currently, the most common approach is to rely on cysteine derivatization. An outline for labeling a small protein with a FRET pair is given in the following:

1. Based on the three-dimensional structure of the protein, remove all solvent-accessible cysteine residues by site-directed mutagenesis and introduce two surface-exposed cysteines with a sequence separation resulting in a clear difference in FRET efficiencies for folded and unfolded protein, respectively.

2. Express the protein, purify it under reducing conditions, and concentrate it to at least 200 μM .
3. Remove the reducing agent and adjust the pH by passing the protein over a desalting column equilibrated with 50 mM sodium phosphate buffer, pH 7.0. Ensure that the resulting protein concentration is at least 100 μM .
4. React the protein with the first chromophore (*see Note 4*) by adding the maleimide derivative of the dye at a 1:1 *M* ratio, incubate 1 h at room temperature or at 4°C overnight.
5. Separate unlabeled, singly labeled, and doubly labeled protein by chromatography, e.g., by ion exchange chromatography, taking advantage of the negative charge on many common chromophores. In favorable cases, this method even allows the separation of labeling permutants (23). Including low concentrations of detergents such as Tween-20 can reduce protein losses resulting from non-specific adsorption to the column material.
6. Concentrate singly labeled protein to at least 100 μM and react with the second chromophore as in points 3 and 4. Make sure that the pH is adjusted properly.
7. Separate singly and doubly labeled protein as in point 5.

Interactions of the dye with the protein surface can interfere both with the photophysics of the chromophores and the stability of the protein. This needs to be taken into account both for the design of the labeled variants and the control experiments. Because of the substantial size of the fluorophores, they can usually only be positioned on the solvent-exposed surface of the protein if the folded structure is to be conserved. Even then, the use of hydrophobic dyes can lead to aggregation of the protein, and interactions with the protein surface can cause a serious reduction in fluorescence quantum yield. Important control experiments are equilibrium or time-resolved fluorescence anisotropy measurements (22,23,33), which are sensitive to the rotational flexibility of the dyes and can therefore provide indications for undesirable interactions with the protein surface. It is also essential to ensure by direct comparison with unmodified protein that labeling has not substantially altered the protein's stability or folding mechanism (22,23).

3.3. Controls

Several factors can complicate single molecule fluorescence experiments, for instance optical saturation and photobleaching, the influence of diffusion, possible interactions of the chromophore with the polypeptide (resulting in a reduction of quantum yields or lack of fast orientational averaging of the dyes), or a change of solvent conditions, which can affect the refractive index and the photophysics and photochemistry of the dyes. A suitably labeled control molecule that essentially provides a rigid spacer between the dyes, and whose conformation does not change under denaturing conditions can thus be valuable for avoiding misinterpretation of the results.

Two suitable types of molecules are double-stranded DNA (13) and polyproline peptides (33). DNA duplexes are very stiff (persistence length of about 50 nm) and can simply be generated by annealing complementary oligonucleotide strands, which are commercially available with fluorophores already attached. For FRET experiments on proteins, however, it is desirable to use a polypeptide-based reference molecule because the type of attachment chemistry and the characteristics of the immediate molecular environment can influence the photophysical properties of the fluorophores (56–58). Additionally, under some conditions used for protein denaturation, a DNA duplex will dissociate. Oligomers of proline in water form a type II helix with a pitch of 0.312 nm per residue and a persistence length of about 5 nm, providing a reasonably stiff spacer (33,59–61). By including an amino terminal glycine residue and a carboxy terminal cysteine residue in the synthesis, the resulting α -amino group and the cysteine's sulfhydryl group can be labeled specifically with derivatives of suitable reactive dyes, such as succinimidyl esters and maleimides, respectively (23,33). Polyproline peptides are therefore suitable reference molecules, but their chain dynamics have to be taken into account, especially for higher oligomers (33).

Another issue that frequently complicates the quantitative analysis of FRET experiments is the orientational factor κ^2 (see **Subheading 1.1.**). Routinely, labeled protein samples should be analyzed with equilibrium or time-resolved fluorescence anisotropy measurements. Low anisotropy values are indicative of freely rotating chromophores; from time-resolved measurements, the rotational correlation time of the dyes can be determined directly (62).

In general, it is always essential to compare the results from single molecule experiments quantitatively with ensemble data (see **Note 5**). Even though it may be tempting to analyze only the results from a few selected molecules, the overall result must agree with the ensemble measurement, and the criteria for singling out molecules for analysis have to be as objective and clearly defined as possible.

3.4. Other Technical Details

3.4.1. Filters

Customizing the single molecule instrument will involve the installation of suitable filters specific for the dye pair used. A compromise between maximum collection efficiency, minimal background from scattering, and cross-talk between the channels (especially donor emission leakage into the acceptor detector) has to be established. At least two dichroic mirrors are required, but the signal-to-noise ratio can usually be improved by additional filters, e.g., long-pass filters to reject scattered laser light, a laser line filter, and band-pass or long-pass filters for the individual detection channels. A broad range of filters and dichroic

mirrors is available from companies such as Chroma or Omega Optical. Other variables involve the choice of excitation intensity and laser pulse frequency (which should be optimized carefully by systematic variation), the objective used (e.g., water immersion vs oil immersion [*see Note 6*]) and the size of the pinhole in a confocal setup.

3.4.2. Cover Glasses

Cells for single molecule measurements are usually assembled using glass cover slides with a thickness corresponding to the optical correction of the objective. Generally, fused silica results in lower background because of the high purity of the material. Impurities on the surface of cover slides can give rise to background, especially in experiments on immobilized molecules close to the surface of the glass. It can thus be crucial to clean them carefully. A wide variety of cleaning methods for cover slides are applied, e.g.,

1. Rubbing the glass carefully with acetone or isopropanol and rinsing.
2. Heating to 500°C or more with a flame or in a suitable oven.
3. Sonicating in a 1:1:5 mixture of 30% ammonium hydroxide, 30% hydrogen peroxide, and water.
4. Etching with a 10% solution of hydrofluoric acid in water for 5 min. (Hydrofluoric acid needs to be handled very carefully. The surface of the polished glass is degraded by etching, and the cover slide can usually not be reused, which is a disadvantage especially for expensive fused silica cover slides.)

3.4.3. Oxygen

The observation time of immobilized single molecules is ultimately limited by photobleaching, an intrinsic property of all organic dyes. Photobleaching is typically a result of excited state (probably triplet state) reactions with highly reactive molecules in solution, such as singlet oxygen. At the same time, oxygen is an efficient quencher of triplet states, whose population at excitation close to optical saturation can strongly decrease the overall fluorescence intensity. However, it may still be advantageous for some experiments to reduce the oxygen concentration. The popular combination of glucose oxidase and catalase in the presence of glucose (**63**) can obviously not be used under most denaturing conditions, but other methods for generating anaerobic conditions are available (**63**).

3.5. Free Diffusion Experiments

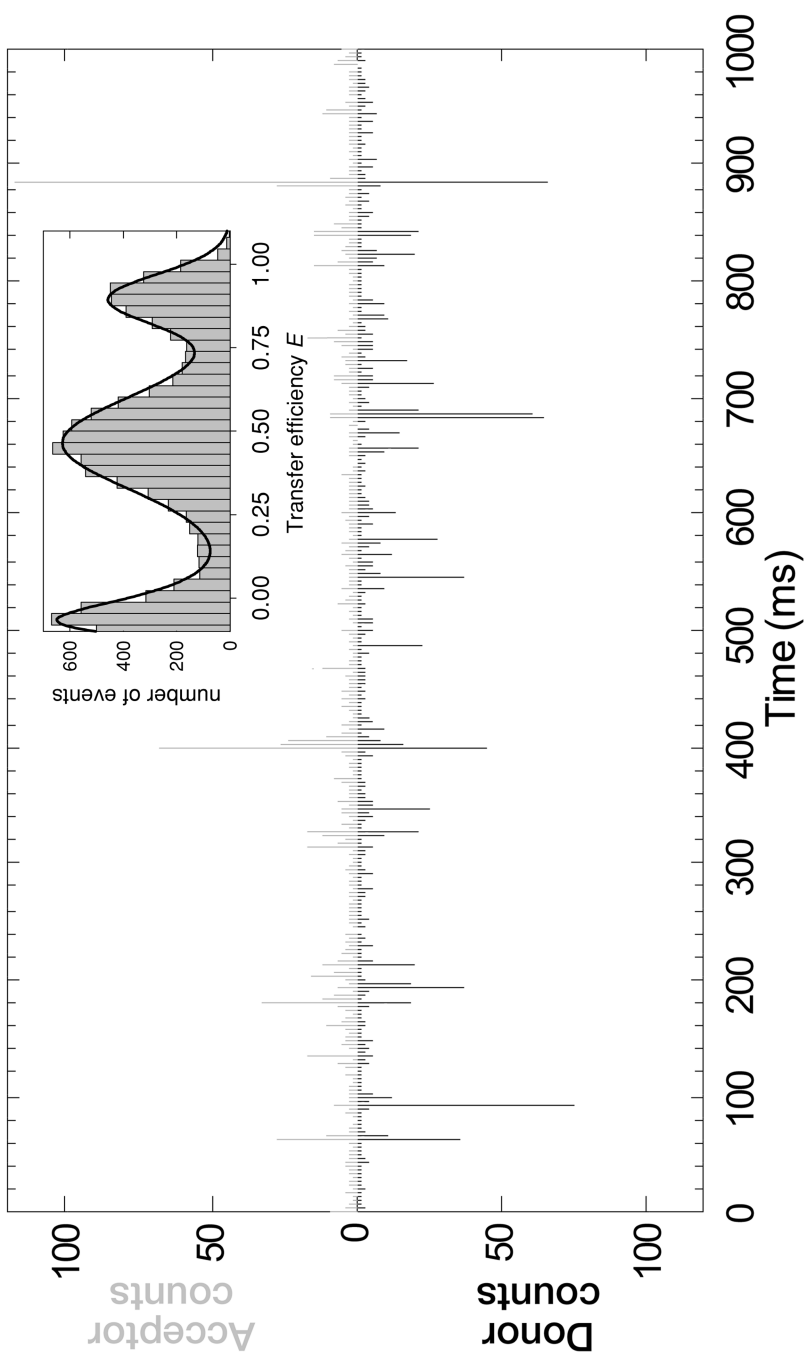
Arguably the simplest single molecule experiment involves diluting a labeled protein sample to a concentration of about 10–100 pM and observing the signal from the confocal excitation and detection volume. In this concentration range, the probability of two protein molecules residing in the confocal volume at the

same time is very small, and the signal bursts observed (**Fig. 4**) arise from individual molecules, provided aggregation can be excluded. As the molecules are only observed for about a millisecond each, bursts from hundreds to thousands of individual molecules are typically collected in several minutes to hours, depending on the protein concentration and the statistics required. The simplest way of analyzing the data is by binning them in intervals approximately equal to the average burst duration, typically about 1 ms. Photon bursts are then identified by a simple threshold criterion, and the counts from contiguous bins above the threshold are summed (31). A slightly more sophisticated approach identifies the beginning and end of photon bursts with higher time resolution, using the corresponding increase and drop in the photon arrival frequency. The counts of a single burst are integrated, and a second threshold for the total number of photons is used to discriminate signal from noise and to select the largest bursts, which is particularly important if fluorescence lifetimes are to be computed from individual bursts (32). Typically, burst sizes between 20 and 200 counts are reached.

Prior to further analysis of the identified bursts, several corrections need to be made. The background must be subtracted from the raw intensities, and the different quantum yields of donor and acceptor, the cross-talk between the channels, and direct excitation of the acceptor need to be taken into account. In the literature, it is common practice to address all of these corrections individually and simply add and subtract the corresponding contributions from each channel. Even though this is sufficient for most practical purposes, it neglects that some of these corrections are interdependent. A more general scheme for the correction of the raw signals is given in **Note 3**. If all parameters are calibrated correctly, the results from the number of emitted photons (**Eq. 3**) and fluorescence lifetimes (**Eq. 4**) should be in agreement.

The lifetimes and corrected photon counts obtained from the individual bursts can then be analyzed in histograms of transfer efficiencies, distances, polarization,

Fig. 4. (Opposite page) Example of data from an experiment on fluorescently labeled CspTm molecules (23) freely diffusing in a solution containing 1.5 M guanidinium chloride conditions close to the unfolding midpoint. One second of a fluorescence intensity measurement (total acquisition time 600 s) is shown, with large bursts of photons originating from individual molecules diffusing through the confocal volume. A histogram of transfer efficiencies calculated for the individual bursts from the entire measurement is shown in the inset. The histogram shows transfer efficiencies of $E \approx 0.9$ for folded and $E \approx 0.4$ for unfolded molecules. This allows changes in transfer efficiencies to be analyzed individually for the two subpopulations (see **Note 7** for the peak at $E \approx 0$ and **Note 8** for the width of the distributions). The measurement was done on a MicroTime 200 time-resolved fluorescence microscope (PicoQuant) with an excitation wavelength of 470 nm.



or burst size distributions, to name just a few examples (**Fig. 4**). In many cases, it is helpful to investigate the relation between several of these parameters, for instance in 2D histograms of fluorescence lifetime vs the transfer efficiency calculated from **Eq. 3**. As a type of 2D spectroscopy, this can lead to better separation of subpopulations or the identification of unique signatures for certain conformational states.

3.6. Experiments on Immobilized Proteins

An approach to observing individual proteins for an extended period of time is their immobilization on a surface. However, nonspecific interactions with the surface can easily disturb the folding reaction (21). Strategies for minimizing such interactions include the optimization of surface functionalization (26,64) or the encapsulation of individual protein molecules in surface-tethered lipid vesicles (27,28,65). Both methods have allowed the observation of single molecule protein folding reactions. The absence of binding to the surface can be tested by single molecule polarization measurements (27,28,65) or by quantitative comparison with experiments on freely diffusing molecules.

For immobilization experiments it can be helpful to prepare a small flow cell that allows rapid buffer exchange, the deposition of materials on the surface, and washing steps. Such flow cells can be assembled from two clean cover slides (*see Subheading 3.4.2.*) with double-sided tape, forming a channel several millimeters wide and about 100- μm deep. The following procedure outlines the deposition of labeled protein encapsulated in lipid vesicles (65):

1. Sonicate a 500- μL suspension of 10 mg/mL egg-phosphatidylcholine (PC) and 0.2 mg/mL biotinylated phosphatidylethanolamine in the buffer to be used for the experiment to create multilamellar vesicles.
2. Extrude part of the suspension through a polycarbonate membrane with 100-nm pores (66) to create large unilamellar vesicles (LUVs), and repeat the procedure with the remaining sample, with about 1 μM of the protein to be encapsulated added to the suspension. This will result in statistical trapping of protein molecules, with the majority of vesicles being empty, and some vesicles containing one and only rarely two or more molecules.
3. Flow empty LUVs into the flow cell and incubate for a few minutes. The vesicles will form a supported bilayer on the surface. Wash the flow cell with buffer.
4. Introduce a solution of 1 mg/mL avidin into the flow cell, which will bind to the biotinylated lipid, and incubate for a few minutes. Wash the flow cell with buffer.
5. Flow in a dilute suspension of the LUVs with encapsulated protein. The vesicles will bind to the surface-adsorbed avidin, unbound vesicles and free protein can be removed by rinsing the flow cell.

Immobilized molecules prepared in this or other ways can be observed either with a confocal system in combination with sample scanning, or by wide field detection with evanescent field excitation. In the former case, the surface is first

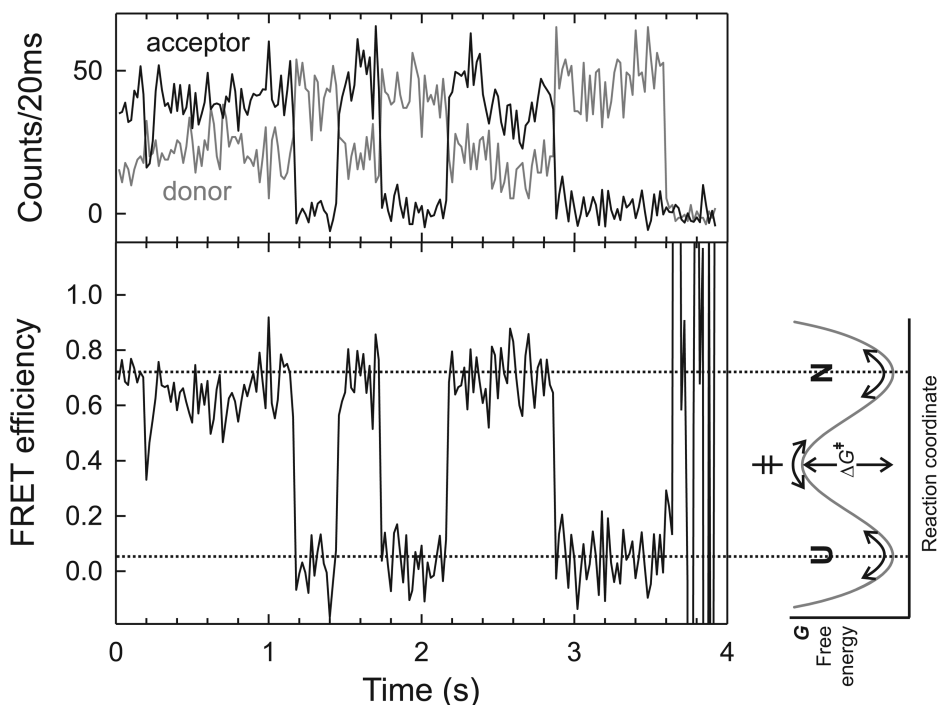


Fig. 5. Example of data from an experiment on fluorescently labeled, vesicle-encapsulated CspTm molecules immobilized on a surface (28). The experiment was performed at 2.0 M guanidinium chloride, the denaturation midpoint of CspTm. Under these conditions, the protein would be expected to remain in the folded and unfolded states for extended periods of time, with rapid, intermittent jumps across the barrier between the two corresponding free energy minima. The top panel shows the fluorescence intensity trajectories recorded from the donor and acceptor chromophores of an individual protein. The anticorrelated changes in their emission intensities result in clear jumps of the transfer efficiency (bottom panel), reflecting the expected behavior of a two-state protein.

scanned to identify individual molecules, which are then targeted by the laser individually and observed sequentially. In the latter case, the information of all molecules in the field of view is obtained simultaneously, albeit with lower time resolution, and usually with an inferior signal-to-noise ratio. In both cases, trajectories of fluorescence intensities are obtained, terminated by photobleaching of a chromophore, which typically occurs after several milliseconds to seconds, depending on the exciting laser intensity. Transfer efficiencies or other parameters are calculated from the trajectories and corrected in a similar way as for the bursts from freely diffusing molecules (*see Subheading 3.5.*). An important criterion for identifying transitions between states is the anticorrelated signal change between donor and acceptor channels (**Fig. 5**), which is expected for a

change in distance between the chromophores. The resulting trajectories of transfer efficiencies can potentially be analyzed by a wide range of methods pioneered in the field of single channel recording (17).

3.7. Limitations of Single Molecule FRET

The number of photons that can be detected from an individual fluorophore is limited by photobleaching to some 10^5 (under ideal conditions). Roughly 100 photons are needed for a signal-to-noise ratio of 10, which means that on the order of up to 1000 observations can be made, in principle sufficient to observe many conformational transitions of a protein. The observation time can be extended by periodically interrupting the laser excitation.

In the other extreme, time resolution is ultimately limited by the photon emission rate, which cannot be greater than the decay rate of the electronically excited state of the chromophores, typically on the order of 10^9 per second. Together with other complications, such as the population of triplet states or low photon collection efficiencies, resolving processes on time-scales of a few microseconds and faster is currently hardly feasible from single events. A possible solution is to make full use of the photon emission statistics from many events, as in fluorescence correlation spectroscopy (FCS) (67) and similar experiments, which have the potential to resolve dynamics on microsecond time-scales (68) and below (69). FCS is a powerful complementary method for studying protein folding dynamics, and as the setup is essentially identical to that of a confocal single molecule instrument, correlations can often be obtained from the same type of measurements as described in **Subheading 3.5**.

How accurately can distances be measured by single molecule FRET? According to **Eq. 1**, the transfer efficiency is most sensitive for distance changes close to R_0 . Theoretically, the precision of a transfer efficiency value determined from a single molecule is only limited by shot noise, i.e., the variation of count rates owing to the quantization of the signal (31,70). For instance, from 100 photons, the standard deviation of E at a distance $r = R_0 = 5$ nm would then be approx 5%, corresponding to an uncertainty in distance of approx 0.2 nm. If more photons are collected or if the signal from many molecules is averaged, a correspondingly higher precision would be achievable. In practice, the presence of background will limit the signal-to-noise ratio and impair the precision—even more so, if the transfer efficiencies are not close to R_0 . In view of the possible systematic errors, especially the uncertainties in the calculation of R_0 (see **Subheading 1.1**), FRET is currently more powerful for detecting distance changes than for accurately measuring absolute distances. However, important advances of the technique are still being made (71,72), and together with a wider variety of reference molecules (33), the accuracy of single molecule FRET measurements will probably be improved further. The study of protein folding will certainly benefit.

4. Notes

1. Note that the equation for R_0 given in the popular textbook of Cantor and Schimmel (73) is not correct.
2. The quantum yield of a chromophore can change upon attachment and must therefore be determined from a protein sample labeled with only one dye.
3. The relation between the raw photon counts $n_{A,0}$ and $n_{D,0}$, as measured in the two detection channels for acceptor and donor emission, respectively, and the corrected values n'_A and n'_D can be expressed by the matrix equation

$$\begin{pmatrix} n_{A,0} \\ n_{D,0} \end{pmatrix} = \begin{pmatrix} a_{11} & a_{12} \\ a_{21} & a_{22} \end{pmatrix} \begin{pmatrix} n'_A \\ n'_D \end{pmatrix} + \begin{pmatrix} b_A \\ b_D \end{pmatrix},$$

where the matrix a_{ij} describes the cumulative effect of the differences in quantum yields, the different collection efficiencies of the detection channels, and cross-talk (“bleed-through”), i.e., acceptor emission detected in the donor channel and donor emission detected in the acceptor channel. b_A and b_D are the background count rates in the acceptor and the donor channel, which can be estimated from a measurement on blank buffer solutions.

The elements of matrix a_{ij} can be determined for a specific single molecule instrument (except for a scaling factor α) from a measurement of two samples containing donor and acceptor dye, respectively, with a concentration ratio equal to the ratio of their extinction coefficients at the excitation wavelength (ensuring that, at identical laser power, the same mean number of excitation events take place per unit time in both samples). By inverting the resulting matrix, the correction matrix $c_{ij} = a_{ij}^{-1}$ is obtained, which transforms the background-corrected raw counts $n_{A,0}-b_A$ and $n_{D,0}-b_D$ into the corrected values n'_A and n'_D . Note that the factor α remains unknown, but cancels if intensity ratios are computed, as in the case of the transfer efficiency. Also note that this correction procedure can easily be extended to more than two channels by using a matrix of higher rank. Finally, n'_A has to be corrected for direct excitation of the acceptor according to, $n_A = n'_A - (n'_A + n'_D)/(1 + \epsilon_D/\epsilon_A)$, where ϵ_D and ϵ_A are the extinction coefficients of donor and acceptor, respectively, at the excitation wavelength. Ideally, these corrections should already be taken into account for burst identification.

4. Adhere to the labeling instructions given by the manufacturer, especially the notes provided by Molecular Probes that are very detailed and helpful.
5. These experiments will take up the great majority of the labeled protein samples, which should be taken into account for the preparation scale.
6. With oil immersion objectives, the focal volume must be positioned very close to the cover slide surface to minimize chromatic aberration. In this case it is particularly important to use fused silica cover slides to reduce background from glass luminescence.
7. The signal from molecules with a transfer efficiency of zero is a notorious phenomenon in free diffusion experiments, which can of course be from incomplete labeling

or impurities, but may also be caused by light-induced inactivation of the acceptor, as suggested by experiments where the sample is flowed (24), but the exact origin of this component of the signal is still a matter of debate. There is no problem if the transfer efficiency of the intact molecules under study is sufficiently different from zero (as in the example of Fig. 3), or if the intact molecules can be separated from the zero transfer events in combination with other observables, such as lifetime or polarization. An elegant general solution is the alternating excitation of donor and acceptor (72,74), which independently probes the acceptor chromophore and allows all molecules with an inactive acceptor to be excluded from the analysis.

8. The width of the transfer efficiency histogram has often been found to be greater than expected from shot noise. This observation has been made on a variety of molecular systems (22,23,33), indicating that additional, unidentified instrumental or physical factors may contribute to the width. Note that a distribution of transfer efficiencies does not necessarily imply a distribution of distances. In this type of measurement, subpopulations with different distances can only be separated if their dynamics are slow on the observation time-scale (in this example milliseconds).

Acknowledgments

This work has been supported by the Deutsche Forschungsgemeinschaft, the VolkswagenStiftung, and the Schweizerischen Nationalfonds. Part of Fig. 3 was provided by Everett Lipman. The author would like to thank Daniel Nettels for discussion, especially concerning data analysis.

References

1. Rief, M., Gautel, M., Oesterhelt, F., Fernandez, J. M., and Gaub, H. E. (1997) Reversible unfolding of individual titin immunoglobulin domains by AFM. *Science* **276**, 1109–1112.
2. Engel, A., Gaub, H. E., and Müller, D. J. (1999) Atomic force microscopy: a forceful way with single molecules. *Curr. Biol.* **9**, R133–R136.
3. Moerner, W. E. (2002) A dozen years of single-molecule spectroscopy in physics, chemistry, and biophysics. *J. Phys. Chem. B* **106**, 910–927.
4. Haustein, E. and Schwille, P. (2004) Single-molecule spectroscopic methods. *Curr. Opin. Struct. Biol.* **14**, 531–540.
5. Michalet, X., Kapanidis, A. N., Laurence, T., et al. (2003) The power and prospects of fluorescence microscopies and spectroscopies. *Annu. Rev. Biophys. Biomol. Struct.* **32**, 161–182.
6. Tamarat, P., Maali, A., Lounis, B., and Orrit, M. (2000) Ten years of single-molecule spectroscopy. *J. Phys. Chem. A* **104**, 1–16.
7. Plakhotnik, T., Donley, E. A., and Wild, U. P. (1997) Single-molecule spectroscopy. *Annu. Rev. Phys. Chem.* **48**, 181–212.
8. Xie, X. S. (1996) Single-molecule spectroscopy and dynamics at room temperature. *Acc. Chem. Res.* **29**, 598–606.

9. Goodwin, P. M., Ambrose, W. P., and Keller, R. A. (1996) Single-molecule detection in liquids by laser-induced fluorescence. *Acc. Chem. Res.* **29**, 607–613.
10. Böhmer, M. and Enderlein, J. (2003) Fluorescence spectroscopy of single molecules under ambient conditions: methodology and technology. *Chem. Phys. Chem.* **4**, 793–808.
11. Haran, G. (2003) Single-molecule fluorescence spectroscopy of biomolecular folding. *J. Physics-Condensed Matter* **15**, R1219–R1317.
12. Förster, T. (1948) Zwischenmolekulare Energiewanderung und Fluoreszenz. *Annalen der Physik* **6**, 55–75.
13. Ha, T., Enderle, T., Ogletree, D. F., Chemla, D. S., Selvin, P. R., and Weiss, S. (1996) Probing the interaction between two single molecules: Fluorescence resonance energy transfer between a single donor and a single acceptor. *Proc. Natl. Acad. Sci. USA* **93**, 6264–6248.
14. Selvin, P. R. (2000) The renaissance of fluorescence resonance energy transfer. *Nature Struct. Biol.* **7**, 730–734.
15. Haas, E., Katchalskikatzir, E., and Steinberg, I. Z. (1978) Brownian-motion of ends of oligopeptide chains in solution as estimated by energy-transfer between chain ends. *Biopolymers* **17**, 11–31.
16. Vix, A. and Lami, H. (1995) Protein fluorescence decay: discrete components or distribution of lifetimes: really no way out of the dilemma. *Biophys. J.* **68**, 1145–1151.
17. Sakmann, B. and Neher, E. (1995) *Single Channel Recording*, Plenum Press, New York, NY.
18. Zhuang, X. and Rief, M. (2003) Single-molecule folding. *Curr. Opin. Struct. Biol.* **13**, 88–97.
19. Kellermayer, M. S., Smith, S. B., Granzier, H. L., and Bustamante, C. (1997) Folding-unfolding transitions in single titin molecules characterized with laser tweezers. *Science* **276**, 1112–1116.
20. Jia, Y. W., Talaga, D. S., Lau, W. L., Lu, H. S. M., DeGrado, W. F., and Hochstrasser, R. M. (1999) Folding dynamics of single GCN4 peptides by fluorescence resonant energy transfer confocal microscopy. *Chem. Phys.* **247**, 69–83.
21. Talaga, D. S., Lau, W. L., Roder, H., et al. (2000) Dynamics and folding of single two-stranded coiled-coil peptides studied by fluorescent energy transfer confocal microscopy. *Proc. Natl. Acad. Sci. USA* **97**, 13,021–13,026.
22. Deniz, A. A., Laurence, T. A., Beligere, G. S., et al. (2000) Single-molecule protein folding: Diffusion fluorescence resonance energy transfer studies of the denaturation of chymotrypsin inhibitor 2. *Proc. Natl. Acad. Sci. USA* **97**, 5179–5184.
23. Schuler, B., Lipman, E. A., and Eaton, W. A. (2002) Probing the free-energy surface for protein folding with single-molecule fluorescence spectroscopy. *Nature* **419**, 743–747.
24. Lipman, E. A., Schuler, B., Bakajin, O., and Eaton, W. A. (2003) Single-molecule measurement of protein folding kinetics. *Science* **301**, 1233–1235.
25. McCarney, E. R., Werner, J. H., Bernstein, S. L., et al. (2005) Site-specific dimensions across a highly denatured protein; a single molecule study. *J. Mol. Biol.* **352**, 672–678.

26. Groll, J., Amirgoulova, E. V., Ameringer, T., et al. (2004) Biofunctionalized, ultrathin coatings of cross-linked star-shaped poly(ethylene oxide) allow reversible folding of immobilized proteins. *J. Am. Chem. Soc.* **126**, 4234–4239.
27. Rhoades, E., Gussakovskiy, E., and Haran, G. (2003) Watching proteins fold one molecule at a time. *Proc. Natl. Acad. Sci. USA* **100**, 3197–3202.
28. Rhoades, E., Cohen, M., Schuler, B., and Haran, G. (2004) Two-state folding observed in individual protein molecules. *J. Am. Chem. Soc.* **126**, 14,686–14,687.
29. Schuler, B. (2005) Single-molecule fluorescence spectroscopy of protein folding. *Chemphyschem*. **6**, 1206–1220.
30. Van Der Meer, BW, Coker, G. III, and Chen, S. Y. S. (1994) *Resonance energy transfer: theory and data*. New York, Weinheim, Cambridge: VCH Publishers, Inc.
31. Deniz, A. A., Laurence, T. A., Dahan, M., Chemla, D. S., Schultz, P. G., and Weiss, S. (2001) Ratiometric single-molecule studies of freely diffusing biomolecules. *Annu. Rev. Phys. Chem.* **52**, 233–253.
32. Eggeling, C., Berger, S., Brand, L., et al. (2001) Data registration and selective single-molecule analysis using multi-parameter fluorescence detection. *J. Biotechnol.* **86**, 163–180.
33. Schuler, B., Lipman, E. A., Steinbach, P. J., Kumke, M., and Eaton, W. A. (2005) Polyproline and the “spectroscopic ruler” revisited with single molecule fluorescence. *Proc. Natl. Acad. Sci. USA* **102**, 2754–2759.
34. Ha, T. (2001) Single-molecule fluorescence resonance energy transfer. *Methods* **25**, 78–86.
35. Moerner, W. E. and Fromm, D. P. (2003) Methods of single-molecule fluorescence spectroscopy and microscopy. *Rev. Sci. Instrum.* **74**, 3597–3619.
36. Wahl, M., Koberling, F., Patting, M., Rahn, H., and Erdmann, R. (2004) Time-resolved confocal fluorescence imaging and spectroscopy system with single molecule sensitivity and sub-micrometer resolution. *Curr. Pharm. Biotechnol.* **5**, 299–308.
37. Hohng, S., Joo, C., and Ha, T. (2004) Single-molecule three-color FRET. *Biophys. J.* **87**, 1328–1337.
38. Clamme, J. -P. and Deniz, A. A. (2005) Three-color single-molecule fluorescence resonance energy transfer. *Chem. Phys. Chem.* **6**, 74–77.
39. Rothwell, P. J., Berger, S., Kensch, O., et al. (2003) Multiparameter single-molecule fluorescence spectroscopy reveals heterogeneity of HIV-1 reverse transcriptase: primer/template complexes. *Proc. Natl. Acad. Sci. USA* **100**, 1655–1660.
40. Williams, R. M., Piston, D. W., and Webb, W. W. (1994) 2-photon molecular-excitation provides intrinsic 3-dimensional resolution for laser-based microscopy and microphotochemistry. *FASEB J.* **8**, 804–813.
41. Margittai, M., Widengren, J., Schweinberger, E., et al. (2003) Single-molecule fluorescence resonance energy transfer reveals a dynamic equilibrium between closed and open conformations of syntaxin 1. *Proc. Natl. Acad. Sci. USA* **100**, 15,516–15,521.
42. Mujumdar, R. B., Ernst, L. A., Mujumdar, S. R., Lewis, C. J., and Waggoner, A. S. (1993) Cyanine dye labeling reagents: sulfoindocyanine succinimidyl esters. *Bioconjug. Chem.* **4**, 105–111.

43. Panchuk-Voloshina, N., Haugland, R. P., Bishop-Stewart, J., et al. (1999) Alexa dyes, a series of new fluorescent dyes that yield exceptionally bright, photostable conjugates. *J. Histochem. Cytochem.* **47**, 1179–1188.
44. Murphy, C. J. (2002) Optical sensing with quantum dots. *Anal. Chem.* **74**, 520A–526A.
45. Chan, W. C., Maxwell, D. J., Gao, X., Bailey, R. E., Han, M., and Nie, S. (2002) Luminescent quantum dots for multiplexed biological detection and imaging. *Curr. Opin. Biotechnol.* **13**, 40–46.
46. Lippitz, M., Erker, W., Decker, H., van Holde, K. E., and Basche, T. (2002) Two-photon excitation microscopy of tryptophan-containing proteins. *Proc. Natl. Acad. Sci. USA* **99**, 2772–2777.
47. Shimomura, O. (2005) The discovery of aequorin and green fluorescent protein. *J. Microsc.* **217**, 1–15.
48. Sako, Y. and Uyemura, T. (2002) Total internal reflection fluorescence microscopy for single-molecule imaging in living cells. *Cell Struct. Funct.* **27**, 357–365.
49. Dawson, P. E. and Kent, S. B. (2000) Synthesis of native proteins by chemical ligation. *Annu. Rev. Biochem.* **69**, 923–960.
50. Ratner, V., Kahana, E., Eichler, M., and Haas, E. (2002) A general strategy for site-specific double labeling of globular proteins for kinetic FRET studies. *Bioconjug. Chem.* **13**, 1163–1170.
51. Kapanidis, A. N. and Weiss, S. (2002) Fluorescent probes and bioconjugation chemistries for single-molecule fluorescence analysis of biomolecules. *J. Chem. Phys.* **117**, 10,953–10,964.
52. David, R., Richter, M. P., and Beck-Sickinger, A. G. (2004) Expressed protein ligation. Method and applications. *Eur. J. Biochem.* **271**, 663–677.
53. Schuler, B. and Pannell, L. K. (2002) Specific labeling of polypeptides at amino-terminal cysteine residues using Cy5-benzyl thioester. *Bioconjug. Chem.* **13**, 1039–1043.
54. Yamaguchi, J., Nemoto, N., Sasaki, T., et al. (2001) Rapid functional analysis of protein-protein interactions by fluorescent C-terminal labeling and single-molecule imaging. *FEBS Lett.* **502**, 79–83.
55. Cropp, T. A. and Schultz, P. G. (2004) An expanding genetic code. *Trends Genet.* **20**, 625–630.
56. Hillisch, A., Lorenz, M., and Diekmann, S. (2001) Recent advances in FRET: distance determination in protein-DNA complexes. *Curr. Opin. Struct. Biol.* **11**, 201–207.
57. Norman, D. G., Grainger, R. J., Uhrin, D., and Lilley, D. M. (2000) Location of cyanine-3 on double-stranded DNA: importance for fluorescence resonance energy transfer studies. *Biochemistry* **39**, 6317–6324.
58. Clegg, R. M., Murchie, A. I., Zechel, A., and Lilley, D. M. (1993) Observing the helical geometry of double-stranded DNA in solution by fluorescence resonance energy transfer. *Proc. Natl. Acad. Sci. USA* **90**, 2994–2998.
59. Stryer, L. and Haugland, R. P. (1967) Energy transfer: a spectroscopic ruler. *Proc. Natl. Acad. Sci. USA* **58**, 719–726.

60. Cowan, P. M. and McGavin, S. (1955) Structure of poly-L-proline. *Nature* **176**, 501–503.
61. Schimmel, P. R. and Flory, P. J. (1967) Conformational energy and configurational statistics of poly-L-proline. *Proc. Natl. Acad. Sci. USA* **58**, 52–59.
62. Lakowicz, J. R. (1999) *Principles of Fluorescence Spectroscopy*. Kluwer Academic/Plenum Publishers, New York, NY.
63. Englander, S. W., Calhoun, D. B., and Englander, J. J. (1987) Biochemistry without oxygen. *Anal. Biochem.* **161**, 300–306.
64. Amirkoulova, E. V., Groll, J., Heyes, C. D., et al. (2004) Biofunctionalized polymer surfaces exhibiting minimal interaction towards immobilized proteins. *Chem. Phys. Chem.* **5**, 552–555.
65. Boukobza, E., Sonnenfeld, A., and Haran, G. (2001) Immobilization in surface-tethered lipid vesicles as a new tool for single biomolecule spectroscopy. *J. Phys. Chem. B* **105**, 12,165–12,170.
66. MacDonald, R. C., MacDonald, R. I., Menco, B. P., Takeshita, K., Subbarao, N. K., and Hu, L. R. (1991) Small-volume extrusion apparatus for preparation of large, unilamellar vesicles. *Biochim. Biophys. Acta* **1061**, 297–303.
67. Frieden, C., Chattopadhyay, K., and Elson, E. L. (2002) What fluorescence correlation spectroscopy can tell us about unfolded proteins. *Adv. Protein Chem.* **62**, 91–109.
68. Chattopadhyay, K., Elson, E. L., and Frieden, C. (2005) The kinetics of conformational fluctuations in an unfolded protein measured by fluorescence methods. *Proc. Natl. Acad. Sci. USA* **102**, 2385–2389.
69. Berglund, A. J., Doherty, A. C., and Mabuchi, H. (2002) Photon statistics and dynamics of fluorescence resonance energy transfer. *Phys. Rev. Lett.* **89**, 068101.
70. Gopich, I. V. and Szabo, A. (2005) Theory of photon statistics in single-molecule Förster resonance energy transfer. *J. Chem. Phys.* **122**, 14,707.
71. Kapanidis, A. N., Lee, N. K., Laurence, T. A., Doose, S., Margeat, E., and Weiss, S. (2004) Fluorescence-aided molecule sorting: Analysis of structure and interactions by alternating-laser excitation of single molecules. *Proc. Natl. Acad. Sci. USA* **101**, 8936–8941.
72. Kapanidis, A. N., Laurence, T. A., Lee, N. K., Margeat, E., Kong, X., and Weiss, S. (2005) Alternating-Laser Excitation of Single Molecules. *Acc. Chem. Res.* **38**, 523–533.
73. Cantor, C. R. and Schimmel, P. R. (1980) *Biophysical Chemistry*, W. H. Freeman and Company, San Francisco, CA.
74. Muller, B. K., Zaychikov, E., Brauchle, C., and Lamb, D. C. (2005) Pulsed Interleaved Excitation. *Biophys. J.* **89**, 3508–3522.
75. Kremer, W., Schuler, B., Harrieder, S., et al. (2001) Solution NMR structure of the cold-shock protein from the hyperthermophilic bacterium *Thermotoga maritima*. *Eur. J. Biochem.* **268**, 2527–2539.